AMBISONICS SYMPOSIUM 2009
June 25-27, Graz

DIGITAL EQUALIZATION FILTERS FOR A SPHERICAL LOUDSPEAKER ARRAY

Alexander Mattioli Pasqual[1], José Roberto de França Arruda[1], Philippe Herzog[2]

[1] Unicamp - VibroAcoustic Laboratory - Campinas, Brazil (pasqual@fem.unicamp.br, arruda@fem.unicamp.br)
[2] CNRS - Laboratoire de Mécanique et d'Acoustique - Marseille, France (herzog@lma.cnrs-mrs.fr)

Abstract: *A spherical loudspeaker array can be used to achieve directivity control. This is carried out by setting the relative voltages of the array elements. In addition, since both the transducer response and the radiation efficiency depend on frequency, equalization filtering must be accomplished in order to produce a flat response. In this work, IIR equalization filters are derived for generating radiation patterns that correspond to the acoustic radiation modes of the array. The voltages and velocities of the transducers are related by using an electrodynamical loudspeaker model based on the Thiele-Small approach. The sound radiation from the loudspeaker array is modeled analytically by considering it as a set of spherical caps mounted on a rigid sphere. A numerical example is presented and it is shown that the acoustic radiation modes are eigenvectors of the transduction matrix when the transducers share an empty enclosure, so that the filter design is simplified.*

Key words: Spatial audio, spherical loudspeaker arrays, equalization filters, directivity control, acoustic radiation modes

1 INTRODUCTION

In the last years, some research on the radiation control by a compact array of independently programmable loudspeakers has been carried out, notably spherical loudspeaker arrays, see [1, 2, 3, 4, 5, 6, 7, 8].

Directivity control can be achieved by setting the relative voltages of the array elements. The control strategy generally adopted is to provide the spherical array with some preprogrammed basic directivities corresponding to spherical harmonic patterns. Then, different directivities can be achieved simply by changing the gains associated with the basic directivities, so that it is not necessary to redesign the filters when a different target directivity pattern is desired.

Acoustic radiation modes (ARMs) are an alternative to spherical harmonics for describing the sound field that a vibrating structure radiates. Such a modal approach is based on how efficiently a given velocity distribution on the structure surface radiates sound energy and it has been used since the 1990's, e.g., [9, 10, 11, 12].

Besides directivity control, since both the transducer response and the radiation efficiency depend on frequency, a spherical loudspeaker array must be provided with a set of equalization filters in order to produce a flat response. In this work, equalizers are derived analytically for generating radiation patterns that correspond to the ARMs of the array. Two equalization approaches are presented and compared. In the first one, sound pressure equalization in a given radiation direction is provided. In the second approach, sound power equalization is provided.

To evaluate the filters, the sound radiation from the spherical array is modeled analytically by considering it as a set of spherical caps mounted on a rigid sphere and by letting each cap oscillate with a constant radial velocity [6]. The voltages that feed the transducers are obtained by the electrodynamical loudspeaker model described in [7]. These models are revisited in this work and a numerical example is provided.

2 SOUND RADIATION

This work concerns the linear acoustic radiation by spherical sources in the frequency domain, so that the Helmholtz equation in spherical coordinates governs the sound propagation. This equation is separable in such a coordinate system and the angular dependence of the solution is given by spherical harmonic functions. Throughout this work a harmonic time dependence of the form $e^{-j\omega t}$ is assumed but is omitted in the notation.

Acoustic radiation modes are vibration patterns that constitute a useful representation of the dynamical behavior of a vibrating structure when one is mainly interested in the sound field that it radiates. Such a modal decomposition is only a function of the frequency and the radiating structure geometry, i.e., it does not depend on the source of excitation and on physical characteristics of the structure, such as material properties and thickness.

This section provides some background on ARMs applied to vibroacoustic sources having a finite number of degrees of freedom. In addition, the radiation model for a spherical loudspeaker array described in [6] is briefly revisited.

2.1. Acoustic radiation modes

The calculation of the acoustic power, W, radiated by a vibrating structure with L degrees of freedom generally leads to expressions of the form (cf. [9, 10, 11, 12])

$$W(\mathbf{u}) = \rho c S \mathbf{u}^{\mathbf{T}} \mathbf{C} \mathbf{u} \tag{1}$$

where ρ is the density of the medium, c is the sound speed, S is the vibrating surface area, $\mathbf{u} \in \mathbb{R}^L$ is the surface velocity of the vibrating structure (here, only real modes are concerned) and $\mathbf{C} \in \mathbb{R}^{L \times L}$ is a coupling matrix, which is symmetric and positive-definite. Throughout this paper, lower case bold letters indicate vectors, while upper case bold letters indicate matrices.

The acoustical radiation efficiency, σ, of a vibroacoustic source is

$$\sigma(\mathbf{u}) = \frac{W(\mathbf{u})}{\rho c S \langle |u|^2 \rangle} \tag{2}$$

where $\langle |u|^2 \rangle$ is the spatial mean-square velocity, i.e., [12]

$$\langle |u|^2 \rangle = \frac{1}{2S} \int_S |u|^2 \, dS = \mathbf{u}^{\mathbf{T}} \mathbf{V} \mathbf{u} \tag{3}$$

where $\mathbf{V} \in \mathbb{R}^{L \times L}$ is symmetric and positive-definite.

Substitution of Eqs.(1) and (3) into (2) yields to

$$\sigma(\mathbf{u}) = \frac{\mathbf{u}^{\mathbf{T}} \mathbf{C} \mathbf{u}}{\mathbf{u}^{\mathbf{T}} \mathbf{V} \mathbf{u}} \tag{4}$$

Since the radiation efficiency is in the form of the generalized Rayleigh quotient, the matrix $\mathbf{V}^{-1}\mathbf{C}$ has L orthogonal eigenvectors $\boldsymbol{\psi}_1, \boldsymbol{\psi}_2, \ldots, \boldsymbol{\psi}_L$ corresponding to the real eigenvalues $\sigma_1 \geq \sigma_2 \geq, \ldots, \geq \sigma_L$, and $\sigma(\boldsymbol{\psi}_l) = \sigma_l$. These eigenvectors constitute the desired ARMs and the eigenvalues are their radiation efficiency coefficients, so that an arbitrary surface velocity can be expressed as

$$\mathbf{u} = \boldsymbol{\Psi} \mathbf{c} \tag{5}$$

where $\boldsymbol{\Psi} \in \mathbb{R}^{L \times L}$ is a matrix that contains the eigenvectors as columns and $\mathbf{c}$ contains nondimensional coefficients.

2.2. Spherical loudspeaker array

The sound radiation from a loudspeaker mounted on a rigid sphere can be approximated by modeling the loudspeaker diaphragm as a spherical cap that oscillates with a constant radial velocity over its surface [6, 13]. This model better approaches the actual loudspeaker sound field as the aperture angle of the cap is made smaller. Therefore, in this work, a spherical loudspeaker array having L transducers is modeled as a vibrating sphere with L degrees of freedom.

Figure 1 illustrates a spherical cap mounted on a rigid sphere, where $(\mathbf{y}, \mathbf{z})$ are global Cartesian coordinates, $\mathbf{r_c}$ is the position vector of the center of the cap, $\mathbf{r_p}$ is the position vector of a given but arbitrary point outside the sphere, θ_0 is the aperture angle of the cap, θ_l is the elevation angle in local coordinates and θ is the elevation angle in global coordinates.

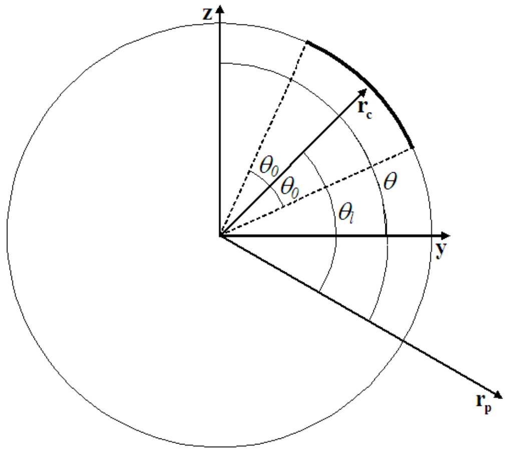

Figure 1: Spherical cap with aperture angle θ_0 mounted on a rigid sphere at $\mathbf{r_c}$.

Now, let the cap oscillate with a constant radial velocity u_l over its surface. Hence, by truncating the series up to order N, the free-field sound pressure (in local coordinates) radiated by the cap is [14]

$$\hat{p}_l(r, \theta_l) = \frac{j \rho c u_l}{2} \sum_{n=0}^{N} [P_{n-1}(\cos\theta_0) - P_{n+1}(\cos\theta_0)] \times \frac{h_n(kr)}{h_n'(ka)} P_n(\cos\theta_l) \tag{6}$$

where $j = \sqrt{-1}$, $P_n(x)$ is the Legendre polynomial of degree n, $h_n(x)$ is the spherical Hankel function of first kind and order n, k is the wave number and a is the sphere radius. For $n = 0$, the difference of Legendre polynomials is just $1 - \cos\theta_0$.

If the spherical array has L loudspeakers, the sound pressure it generates will be obtained by superimposing the radiated fields from the L caps, i.e.,

$$p(r, \theta, \varphi) = \sum_{l=1}^{L} p_l(r, \theta, \varphi) \tag{7}$$

where φ is the azimuth angle and p_l is the sound pressure produced by the l-th cap in global coordinates.

3 TRANSDUCER MODELING

An electroacoustic model of the loudspeaker array can be used for evaluating the voltages that must feed the transducers in order to achieve the velocities corresponding to the ARMs of the array.

Here, only electrodynamical loudspeakers are concerned. Figure 2 is a free body diagram of the n-th spherical cap of the loudspeaker array. It is worth noting that the spherical cap represents the driver diaphragm assembly including voice coil. There are mechanical (F_{Mn}), acoustical (F_{In} and F_{En}) and electromagnetical (F_{Ln}) forces acting on it. F_{Mn} is due to the moving mass of the n-th driver, as well as the compliance and resistance of its suspension. F_{In} and F_{En} arise from the sound pressure fluctuation inside and outside the spherical array, respectively. F_{Ln} is the Lorentz force.

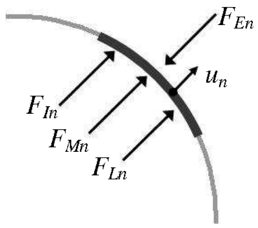

Figure 2: Free body diagram of the n-th spherical cap of the array.

Application of the second Newton's law in the n-th transducer yields to

$$F_{In} + F_{Mn} + F_{Ln} = F_{En} \tag{8}$$

Following [7], F_{Mn} and F_{Ln} can be evaluated by using a simple lumped parameter model based on the Thiele-Small approach, so that

$$F_{Mn} = -Z_{Mn}u_n = \left(j\omega M_n - R_n + \frac{1}{j\omega C_n}\right)u_n \tag{9}$$

and

$$F_{Ln} = \frac{(BL)_n}{R_{En}}v_n - \frac{(BL)_n^2}{R_{En}}u_n \tag{10}$$

where ω is the angular frequency, Z_{Mn} is the mechanical impedance of the n-th driver, M_n is the moving mass of the n-th driver, R_n is the mechanical resistance of the n-th driver suspension, C_n is its mechanical compliance, $(BL)_n$ is the force factor of the n-th driver, v_n is its voltage and R_{En} is the electrical resistance of the n-th voice-coil. The relation between these parameters and the well-known Thiele-Small parameters can be easily found in the literature. See, for example, [15].

In this work, it is assumed that the transducers of the array are mounted on an empty cavity, i.e., the drivers share a common enclosure so that there is an internal acoustic coupling between them. At low frequencies, when high-order modes do not propagate inside the cavity, the enclosure can be modeled as an acoustic compliance, so that F_{In} becomes [7]

$$F_{In} = \sum_{l=1}^{L}\frac{S_nS_l}{j\omega C_B}u_l \tag{11}$$

where S_l is the effective radiation area of the l-th driver and C_B is the acoustic compliance of the enclosure, which is given by [15]

$$C_B = \frac{V_B}{\rho c^2} \tag{12}$$

where V_B is the volume of the cavity.

On the other hand, at high frequencies, the diaphragm displacement is small yielding to irrelevant volume changes, so that F_{In} can be neglected. However, controllability problems will take place at the natural frequencies of the cavity. Anyway, since these frequencies for a spherical cavity are easy to evaluate, there is no need to use a complex enclosure model in order to identify them. For further details and a discussion about the enclosure design for a loudspeaker array, see [7].

F_{En} has a minor effect on the voltages when free-field radiation is concerned. Thus, in order to evaluate F_{En}, it is assumed that each transducer radiates as a piston mounted on an infinite baffle. In addition, the external coupling between drivers is ignored [7]. Then,

$$F_{En} = Z_{Rn}S_n^2u_n \tag{13}$$

where Z_{Rn} is the radiation impedance of a circular piston mounted on an infinite baffle corresponding to the n-th driver. A mathematical expression for Z_{Rn} can be found in [16].

Substitution of Eqs.(9), (10), (11) and (13) into (8) yields to

$$\left(Z_{Mn} + \frac{(BL)_n^2}{R_{En}} + Z_{Rn}S_n^2\right)u_n - \sum_{l=1}^{L}\frac{S_nS_l}{j\omega C_B}u_l = \frac{(BL)_n}{R_{En}}v_n \tag{14}$$

Equation (14) can be written in the matrix form as follows

$$\mathbf{Zu} = \mathbf{v} \tag{15}$$

where $\mathbf{v} \in \mathbb{C}^L$ contains the complex amplitude of the voltages that feed the transducers and $\mathbf{Z} \in \mathbb{C}^{L\times L}$. If all drivers of the array have the same electroacoustic characteristics, $\mathbf{Z}$ becomes

$$\mathbf{Z}(\omega) = f(\omega)\,\mathbf{1} + g(\omega)\,\mathbf{I} \tag{16}$$

where $\mathbf{1}$ is an $L \times L$ matrix of all 1's, $\mathbf{I}$ is the identity matrix of order L,

$$f(\omega) = -\frac{R_E}{BL}\frac{S^2}{j\omega C_B} \tag{17}$$

and

$$g(\omega) = \frac{R_E}{BL}\hat{Z} \tag{18}$$

where $\hat{Z} = Z_{Mn} + \frac{(BL)_n^2}{R_{En}} + Z_{Rn}S_n^2$.

Now, let $\boldsymbol{\eta}$ be an eigenvector of $\mathbf{Z}$ and μ be its corresponding eigenvalue, then

$$\mathbf{Z}(\omega)\,\boldsymbol{\eta} = \mu(\omega)\,\boldsymbol{\eta} \tag{19}$$

Substitution of Eq.(16) into (19) leads to

$$\mathbf{1}\boldsymbol{\eta} = \left(\frac{\mu(\omega) - g(\omega)}{f(\omega)}\right)\boldsymbol{\eta} \tag{20}$$

It is known that the eigenvalues of $\mathbf{1}$ are

$$\frac{\mu(\omega) - g(\omega)}{f(\omega)} = \begin{cases} 0 & \text{multiplicity } L-1 \\ L & \text{multiplicity } 1 \end{cases} \tag{21}$$

Then, substitution of Eq.(21) into (19) leads to the following necessary and sufficient condition for a vector be an eigenvector of **Z**:

$$\sum_{i=1}^{L} \eta_i = 0 \quad \text{or} \quad \eta_1 = \eta_2 = \cdots = \eta_L \tag{22}$$

Finally, Eqs.(21) and (22) lead to

$$\mu(\omega) = \begin{cases} g(\omega) & \text{if } \sum_{i=1}^{L} \eta_i = 0 \\ Lf(\omega) + g(\omega) & \text{if } \eta_1 = \cdots = \eta_L \end{cases} \tag{23}$$

It will be verified later that the ARMs of a spherical dodecahedral loudspeaker array satisfy Eq.(22).

4 EQUALIZATION FILTERING

Let $X(\omega)$ be the Fourier transform of a mono signal which one wants to diffuse trough a spherical loudspeaker array with a directivity corresponding to an ARM of the array, so that $\mathbf{u}(\omega) = \boldsymbol{\psi}_\mathbf{i} X(\omega)$, where $\boldsymbol{\psi}_\mathbf{i} \in \mathbb{R}^L$ is the i-th ARM of the array. In addition, if $\boldsymbol{\psi}_\mathbf{i}$ is assumed to be an eigenvector of **Z**, Eqs.(15) and (19) yield to

$$\mathbf{v_i}(\omega) = \mu_i(\omega)\, \boldsymbol{\psi}_\mathbf{i} X(\omega) \tag{24}$$

A block diagram is shown in Fig.(3). It is worth noting that each element of the matrix $\boldsymbol{\Psi}$ is a real number.

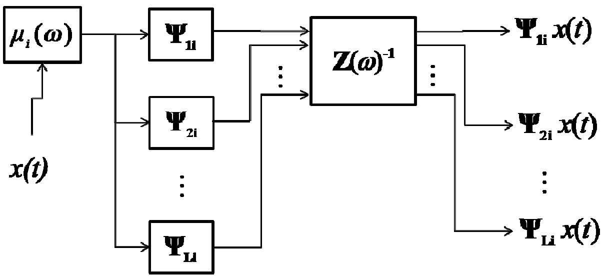

Figure 3: Block diagram representing the synthesis of the i-th ARM of a L-driver loudspeaker array.

The i-th ARM can be achieved by multiplying the input electrical signal by a set of L real numbers given in $\boldsymbol{\psi}_\mathbf{i}$. Driver velocity equalization is provided by $\mu_i(\omega)$. However, since radiation efficiency is highly dependent on frequency, additional equalization must be accomplished in order to take it into account. Let $\epsilon_i(\omega)$ be a filter that provides such an extra equalization. Thus, for a complete equalized system, tensions that must feed the drivers are given by

$$\mathbf{v_i}(\omega) = E_i(\omega)\, \boldsymbol{\psi}_\mathbf{i} X(\omega) \tag{25}$$

where

$$E_i(\omega) \equiv \epsilon_i(\omega)\, \mu_i(\omega) \tag{26}$$

Now, let $\mathbf{A}(\mathbf{r_p}, \omega) \in \mathbb{C}^L$ contain the directivities of the loudspeakers of the array evaluated by Eq.(6), i.e., it relates the driver velocities with the sound pressure in $\mathbf{r_p}$, where $|\mathbf{r_p}| \geq a$. Then, the sound pressure field produced by the spherical array when its vibration pattern corresponds to its i-th ARM after equalization is

$$\bar{p}_i(\mathbf{r_p}, \omega) = \mathbf{A}(\mathbf{r_p}, \omega)^\mathbf{T}\, \mathbf{Z}(\omega)^{\mathbf{-1}}\, \boldsymbol{\psi}_\mathbf{i} E_i(\omega)\, X(\omega) \tag{27}$$

A block diagram is shown in Fig.(4).

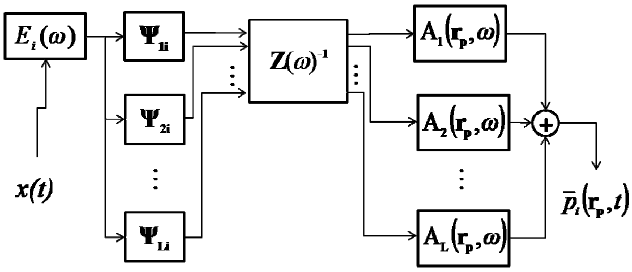

Figure 4: Block diagram representing the sound field produced by the i-th ARM of a L-driver loudspeaker array after equalization.

In this work, the equalization filter $E_i(\omega)$ is approximated by a rational polynomial function in z, i.e.,

$$E_i(z) \approx \frac{\sum_{k=0}^{B} b_k z^{-k}}{\sum_{k=0}^{D} d_k z^{-k}} \tag{28}$$

where $z = e^{-j\omega T_s}$ and T_s is the sampling period.

In the following, two equalization schemes are presented to evaluate $E_i(\omega)$ and, consequently, $\epsilon_i(\omega)$. The first one is based on the sound pressure response in a given radiation direction, and the second one is based on the sound power radiated by the spherical array.

4.1. Sound pressure

The sound pressure field, p_i, produced by a spherical array when the driver tensions are weighted according to $\boldsymbol{\psi}_\mathbf{i}$ is

$$p_i(\mathbf{r_p}, \omega) = \mathbf{A}(\mathbf{r_p}, \omega)^\mathbf{T}\, \mathbf{Z}(\omega)^{\mathbf{-1}}\, \boldsymbol{\psi}_\mathbf{i} X(\omega) \tag{29}$$

Now, let $\hat{\mathbf{r}}_\mathbf{p}$ be a given point in the acoustic domain and $H_i(\omega)$ be a frequency response function defined as

$$\begin{aligned} H_i(\omega) &\equiv \mathbf{A}(\hat{\mathbf{r}}_\mathbf{p}, \omega)^\mathbf{T}\, \mathbf{Z}(\omega)^{\mathbf{-1}}\, \boldsymbol{\psi}_\mathbf{i} \\ &= \mathbf{A}(\hat{\mathbf{r}}_\mathbf{p}, \omega)^\mathbf{T} \frac{1}{\mu_i(\omega)} \boldsymbol{\psi}_\mathbf{i} \end{aligned} \tag{30}$$

$H_i(\omega)$ can be written as the product of a minimum-phase system, $H_i^{(min)}(\omega)$, and an all-pass system, $H_i^{(ap)}(\omega)$, so that [17]

$$H_i(\omega) = H_i^{(min)}(\omega)\, H_i^{(ap)}(\omega) \tag{31}$$

Comparison of Eqs.(27) and (30) shows that sound pressure equalization in the direction $\hat{\mathbf{r}}_\mathbf{p}$ could be achieved by letting $E_i(\omega) = H_i(\omega)^{-1}$. However, this leads to a non-realizable equalizer since the inverse of $H_i^{(ap)}(\omega)$ is non-causal. Fortunately, for the problem considered here, it will be seen that $H_i^{(ap)}(\omega)$ is approximately a pure delay system, so that it does not provide phase distortion. Thus, a

$$
\mathbf{\Psi} = \begin{bmatrix}
0.2887 & 0.5 & 0 & 0 & 0.6455 & 0 & 0 & 0 & 0 & 0 & 0 & 0.5 \\
0.2887 & 0.2236 & 0.4472 & 0 & -0.1291 & 0.4472 & 0.4472 & 0 & 0 & 0.4472 & 0 & -0.2236 \\
0.2887 & 0.2236 & 0.1382 & 0.4253 & -0.1291 & -0.3618 & 0.1382 & 0.4253 & -0.2629 & -0.3618 & -0.2629 & -0.2236 \\
0.2887 & 0.2236 & -0.3618 & 0.2629 & -0.1291 & 0.1382 & -0.3618 & 0.2629 & 0.4253 & 0.1382 & 0.4253 & -0.2236 \\
0.2887 & 0.2236 & -0.3618 & -0.2629 & -0.1291 & 0.1382 & -0.3618 & -0.2629 & -0.4253 & 0.1382 & -0.4253 & -0.2236 \\
0.2887 & 0.2236 & 0.1382 & -0.4253 & -0.1291 & -0.3618 & 0.1382 & -0.4253 & 0.2629 & -0.3618 & 0.2629 & -0.2236 \\
0.2887 & -0.2236 & -0.4472 & 0 & -0.1291 & 0.4472 & 0.4472 & 0 & 0 & -0.4472 & 0 & 0.2236 \\
0.2887 & -0.2236 & -0.1382 & -0.4253 & -0.1291 & -0.3618 & 0.1382 & 0.4253 & -0.2629 & 0.3618 & 0.2629 & 0.2236 \\
0.2887 & -0.2236 & 0.3618 & -0.2629 & -0.1291 & 0.1382 & -0.3618 & 0.2629 & 0.4253 & -0.1382 & -0.4253 & 0.2236 \\
0.2887 & -0.2236 & 0.3618 & 0.2629 & -0.1291 & 0.1382 & -0.3618 & -0.2629 & -0.4253 & -0.1382 & 0.4253 & 0.2236 \\
0.2887 & -0.2236 & -0.1382 & 0.4253 & -0.1291 & -0.3618 & 0.1382 & -0.4253 & 0.2629 & 0.3618 & -0.2629 & 0.2236 \\
0.2887 & -0.5 & 0 & 0 & 0.6455 & 0 & 0 & 0 & 0 & 0 & 0 & -0.5
\end{bmatrix}
$$

Figure 5: ARMs of a spherical array with $L = 12$ and $\theta_0 = 15.86^0$.

system with linear phase and no pressure magnitude distortion in the direction $\hat{\mathbf{r}}_\mathbf{p}$ can be obtained by letting

$$E_i(\omega) = \frac{1}{H_i^{(min)}(\omega)} \quad (32)$$

Since $E_i(\omega)$ is a minimum-phase system, the coefficients in Eq.(28) can be obtained by using an IIR filter design method which approximates a given but arbitrary magnitude response. In order to ensure that approximated $E_i(\omega)$ is a minimum-phase system, its poles and zeros must be inside the unit circle in the z-plane.

4.2. Sound power

The equalization schema described in the previous section is limited to a given radiation direction. This can be dealt with by equalizing the sound power radiated by the array instead of the sound pressure in a given radiation direction.

Consider Fig.(4), the diaphragm velocities corresponding to the i-th ARM can be seen to be

$$\mathbf{u}(\omega) = \mathbf{Z}(\omega)^{\mathbf{-1}} \boldsymbol{\psi}_\mathbf{i} E_i(\omega) X(\omega) = \boldsymbol{\psi}_\mathbf{i} \frac{E_i(\omega)}{\mu_i(\omega)} X(\omega) \quad (33)$$

If the L transducers of the spherical array have the same diaphragm area, which are modeled as spherical caps, one has

$$S = 2\pi a^2 (1 - \cos\theta_0) L \quad (34)$$

By normalizing the ARMs so that $\boldsymbol{\psi}_i^\mathbf{T} \boldsymbol{\psi}_i = 1$, substitution of Eq.(33) into (3) yields to

$$\langle |u|^2 \rangle = \frac{1}{2L} \frac{|E_i(\omega)|^2}{|\mu_i(\omega)|^2} |X(\omega)|^2 \quad (35)$$

Since $\sigma(\mathbf{u}) = \sigma(\boldsymbol{\psi}_\mathbf{i}) = \sigma_i(\omega)$, substitution of Eqs.(34) and (35) into (2) leads to

$$W_i = \sigma_i(\omega) \rho c \pi a^2 (1 - \cos\theta_0) \frac{|E_i(\omega)|^2}{|\mu_i(\omega)|^2} |X|^2 \quad (36)$$

Finally, for a unitary gain, the magnitude response of the equalizer must be

$$|E_i(\omega)| = \frac{|\mu_i(\omega)|}{\sqrt{\sigma_i(\omega) \rho c \pi a^2 (1 - \cos\theta_0)}} \quad (37)$$

Since only magnitude response is concerned in Eq.(37), the coefficients in Eq.(28) can be obtained by using an IIR filter design method which approximates a given but arbitrary magnitude response.

5 NUMERICAL EXAMPLE AND DISCUSSION

In order to illustrate and to discuss the ideas presented in the previous sections, equalization filters for a spherical array with $L = 12$ identical transducers are studied here.

The spherical caps (transducer diaphragm) are distributed over a sphere of radius $a = 0.075m$ according to the dodecahedron symmetry, so that spatial orientation of each one of them is made equal to the vector normal to a face of a dodecahedron. The aperture angle of the caps under consideration is $\theta_0 = 15.86^0$ and the medium properties are assumed to be $c = 343m/s$ and $\rho = 1.21kg/m^3$. The ARMs of such a spherical array are shown in Fig.5. It can be verified that they satisfy Eq.(22), i.e., these ARMs are eigenvectors of **Z**.

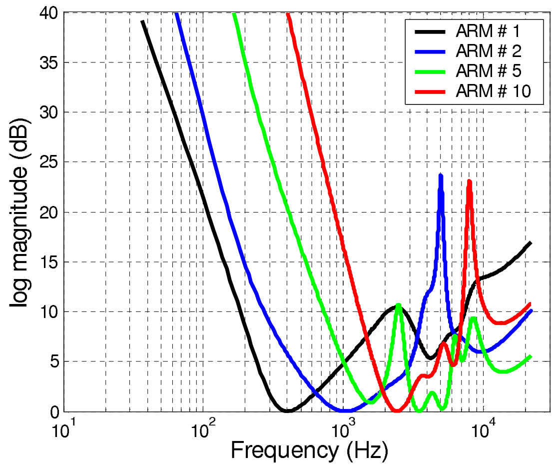

Figure 6: Frequency response of sound pressure equalizers for some ARMs of the spherical array.

In order to evaluate $\mu_i(\omega)$, all transducers are supposed to be equal with the following characteristics: $2in$ drivers, resonance frequency $200Hz$, mechanical quality factor 4.72, electrical quality factor 0.80, total moving mass $0.00104kg$, $R_{En} = 6.4\Omega$ and $S_n = 0.00132m^2$.

$\mathbf{A}(\mathbf{r_p}, \omega)$ is evaluated by truncating the series given in Eq.(6) to order $N = 10$ and letting $|\mathbf{r_p}| = 20a = 1.5m$, i.e., it defines a spherical surface in the far-field. In addition, $\hat{\mathbf{r}}_\mathbf{p}$ is chosen so that it corresponds to the main radiation direction of the array in the low frequency range. Thus, the frequency response of the sound pressure equalizers evaluated by Eqs.(32) and (30) for some ARMs are shown in Fig.6. Since the directivity of an ARM becomes very complicated at high frequencies, it may happen that $\hat{\mathbf{r}}_\mathbf{p}$ matches a low pressure direction, leading to the high frequency peaks shown in Fig.6.

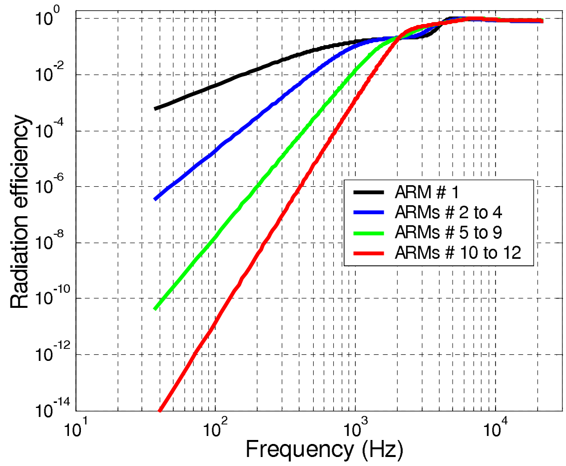

Figure 7: Radiation efficiencies of the ARMs of a spherical array with $a = 0.075m$, $L = 12$ and $\theta_0 = 15.86^0$.

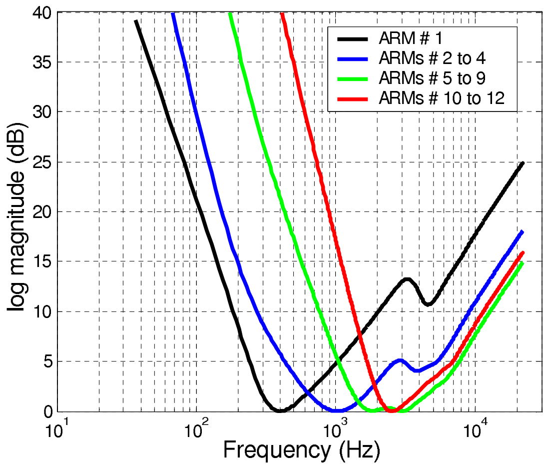

Figure 8: Frequency response of sound power equalizers for the ARMs of the spherical array.

The radiation efficiencies corresponding to each one of the ARMs given in $\mathbf{\Psi}$ are presented in Fig.7, which illustrates the grouping characteristic of the ARMs discussed in [12]. The frequency response of the sound power equalizers evaluated by Eq.(37) are presented in Fig.8.

Comparison of Figs.6 and 8 shows no differences in the frequency responses at low frequencies between pressure equalization and power equalization. However, sound power equalization presents two main advantages at high frequencies. First, since power equalization is not based on a single radiation direction, there are no high frequency peaks. Second, only 4 filters can be used to deal with the 12 ARMs due to their grouping characteristic concerning radiation efficiency.

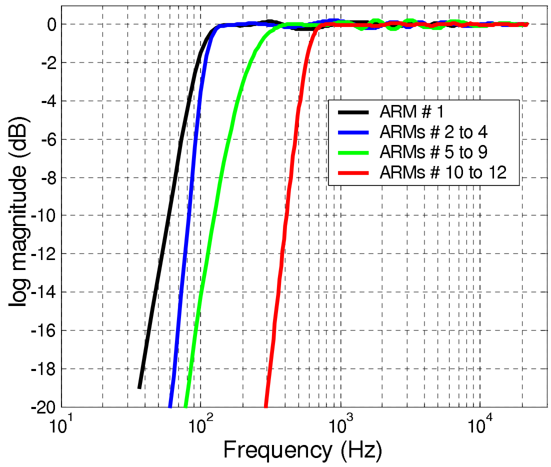

Figure 9: Squared sound power response of the power equalized audio system for the ARMs of the spherical array. IIR equalization filters with $B = D = 9$.

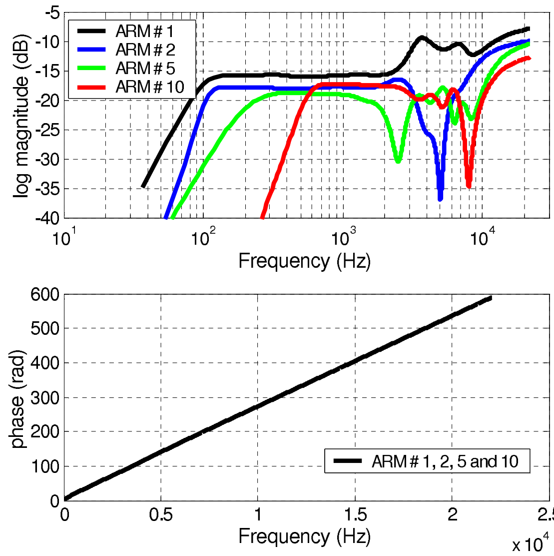

Figure 10: Sound pressure response at $\hat{\mathbf{r}}_\mathbf{p}$ for some ARMs of the spherical array with power equalization. IIR equalization filters with $B = D = 9$.

The MATLAB® filter design toolbox has been used to obtain the coefficients of digital IIR filters that approximate the magnitude frequency response of the sound power equalizers presented in Fig.8. Figure 9 is the log magnitude plot of the squared sound power response when $B = D = 9$ in Eq.(28) and $T_s = (44100)^{-1}\, s$.

Figure 8 shows that the filters must achieve large gain values in order to provide equalization at low frequencies, so that application of such filters can damage the transducers. Therefore, the low frequency response of the equalizers has been neglected when evaluating the IIR coefficients. Then, no equalization is achieved at low frequencies, as shown in Fig.9.

Figure 10 shows the sound pressure response at $\hat{\mathbf{r}}_\mathbf{p}$ for some ARMs of the power equalized system. Phase response is linear, as stated before, i.e., the equalized system does not provide phase distortion in the direction of $\hat{\mathbf{r}}_\mathbf{p}$.

6 CONCLUSION

In this work, equalization filters for the ARMs of a spherical loudspeaker array have been studied. Two equalization approaches have been compared: sound power equalization and sound pressure equalization in a given radiation direction.

Sound power and sound pressure equalizers can be approximated by 9^{th} order IIR digital filters. Both equalization strategies lead to filters with the same frequency response at low frequencies. On the other hand, unlike sound power equalizers, sound pressure equalizers can present peaks in their frequency response at high frequencies due to the very complicated directivity patterns of the ARMs. Therefore, sound power equalization is more suitable than sound pressure equalization. In addition, since the radiation efficiencies of the ARMs present grouping characteristic, sound power equalization yields to a reduced number of filters in comparison with sound pressure equalization, e.g., for a dodecahedron-like array, only 4 sound power equalizers can handle its 12 ARMs, while 12 sound pressure equalizers must be used for the same purpose.

It has also been shown that the ARMs of a spherical dodecahedral loudspeaker array are eigenvectors of the transduction matrix , **Z**, when the drivers are let to share a common enclosure, so that the filter design is simplified.

7 ACKNOWLEDGMENTS

The authors would like to thank CAPES (Coordenação de Aperfeiçoamento de Pessoal de Nível Superior) for the financial support of this work.

REFERENCES

[1] R. Caussé, J. F. Bresciani and O. Warusfel, "Radiation of musical instruments and control of reproduction with loudspeakers", Proceedings of the International Symposium on Musical Acoustics, 1992, Tokyo

[2] P. Dérogis, R. Caussé and O. Warusfel, "On the reproduction of directivity patterns using multi-loudspeaker source", Proceedings of the International Symposium on Musical Acoustics, 1995, Dourdan, France, 387-392

[3] O. Warusfel and N. Misdariis, "Directivity synthesis with a 3D array of loudspeakers: application for stage performance", Proceedings of the COST G-6 Conference on Digital Audio Effects (DAFX-01), 2001, Limerick, Ireland

[4] P. Kassakian and D. Wessel, "Characterization of spherical loudspeaker arrays", Proceedings of the 117th Audio Engineering Society Convention, 2004, San Francisco, Paper Number 6283

[5] R. Avizienis, A. Freed, P. Kassakian and D. Wessel, "A compact 120 independent element spherical loudspeaker array with programmable radiation patterns", Proceedings of the 120th Audio Engineering Society Convention, 2006, Paris, Paper Number 6783

[6] F. Zotter, A. Sontacchi and R. Höldrich, "Modeling a spherical loudspeaker system as multipole source", Proceedings of the 33rd German Annual Conference on Acoustics, 2007, Stuttgart

[7] A. M. Pasqual, J. R. Arruda and P. Herzog, "Effects of enclosure design on the directivity synthesis by spherical loudspeaker arrays", Proceedings of the 2nd ASA-EAA Joint Conference (Acoustics'08), 2008, Paris, 4235-4240

[8] G. K. Behler, "Sound source for the measurement of room impulse responses for auralisation", Proceedings of the 19th International Congress on Acoustics, 2007, Madrid

[9] K. A. Cunefare, "The minimum multimodal radiation efficiency of baffled finite beams", J. Acoust. Soc. Am. 90, 1991, 2521-2529

[10] K. A. Cunefare and M. N. Currey, "On the exterior acoustic radiation modes of structures", J. Acoust. Soc. Am. 96, 1994, 2302-2312

[11] G. V. Borgiotti and K. E. Jones, "Frequency independence property of radiation spatial filters", J. Acoust. Soc. Am. 96, 1994, 3516-3524

[12] K. A. Cunefare, M. N. Currey, M. E. Johnson and S. J. Elliott, "The radiation efficiency grouping of free-space acoustic radiation modes", J. Acoust. Soc. Am. 109, 2001, 203-215

[13] P. M. Morse and K. U. Ingard, *Theoretical Acoustics* (McGraw-Hill), 1968, Chap. 7.2, pp. 332-355

[14] E. G. Williams, *Fourier Acoustics: Sound Radiation and Nearfield Acoustical Holography* (Academic Press), 1999, Chap. 6.7, pp. 206-216

[15] R. H. Small, "Direct-radiator loudspeaker system analysis", J. Audio Engineering Society 20, 1972, 383-395

[16] L. L. Beranek, *Acoustics* (Acoustical Society of America, New York), 1993

[17] A. V. Oppenheim, R. W. Schafer and J. R. Buck, *Discrete-Time Signal Processing* (Prentice Hall, New Jersey), 1999, Chap. 5, pp. 240-339